Oncology Research, Vol. 25, pp. 1517–1527
Printed in the USA.

0965-0407/17 $90.00 + .00
DOI: https://doi.org/10.3727/096504017X14859934460780
E-ISSN 1555-3906
www.cognizantcommunication.com

FOXO1–MALAT1–miR-26a-5p Feedback Loop Mediates Proliferation and Migration in Osteosarcoma Cells

Juntao Wang and Guodong Sun

Department of Traditional Chinese Orthopedics and Traumatology, the Affiliated Hospital of Shandong Academy of Medical Sciences, Jinan, Shandong Province, P.R. China

miR-26a has been found to be downregulated in osteosarcoma (OS) when compared with normal control tissues and has been shown to suppress the malignant behaviors of OS cells. The underlying mechanism, nevertheless, remains unknown. In our study, the long noncoding RNA MALAT1, confirmed to be significantly upregulated in OS, is first shown to be capable of promoting proliferation and migration by directly suppressing miR-26a-5p in OS cells. In addition, we have identified forkhead box O1 (FOXO1) as a transcriptional factor of MALAT1 that can negatively regulate MALAT1. We have shown that MALAT1 promoted growth and migration through inhibiting miR-26a-5p in OS cells. Suppression of FOXO1, identified as a regulatory transcriptional factor of MALAT1, was shown to be able to slow down both proliferation and metastases in OS cells, suggesting that targeting FOXO1 can be useful in the therapy of patients with OS.

Key words: Osteosarcoma (OS); miR-26a-5p; MALAT1; Forkhead box O1 (FOXO1); Metastasis

INTRODUCTION

Osteosarcoma (OS) is the most common primary bone cancer in children and adolescents. Despite the advancement in diagnosis and treatment of OS, the mortality rate remains high, and no significant improvement in survival has been achieved. The survival rate has been estimated to be no more than 50% in patients treated with multidrug chemotherapy and local control interventions[1]. In addition, many patients with OS showed marked resistance to the available chemotherapeutic reagents and then died due to widespread metastasis and tumor relapse, which was a significant obstacle for successful treatments of patients with OS. In consideration of this, there is an urgent need to develop a new and more effective therapy than the conventional ones for the treatment of OS[2,3].

Pathogenesis of OS has been difficult to establish because of its well-known heterogeneous nature[4]. Tumorigenesis of OS has been linked to alterations of several genes[5] that have been reported to be significantly associated with metastasis, prognosis, or treatment resistance. Therefore, candidate molecules such as diagnostic, prognostic, or therapeutic biomarkers/targets were expected to be identified and may thus improve therapeutic efficacy and clinical outcomes for patients with OS. In this setting, long noncoding RNAs (lncRNAs) are emerging as important molecular markers involved in human cancers, including OS[6]. lncRNAs are defined as endogenous RNA longer than 200 nucleotides that do not contain significant open reading frames and thus do not result in proteins[7]. Some lncRNAs have recently been shown to play a key role in OS. MALAT1[6] (metastasis-associated lung adenocarcinoma transcript 1) was one of the lncRNAs among those reported to be involved in OS. MALAT1 has been reported to exert an important role as an lncRNA in OS. Despite the fact that MALAT1 has been shown to be able to promote proliferation and metastasis in OS[8,9], the underlying molecular mechanism behind it remains unknown.

In our study, we have shown that MALAT1 promoted growth and migration of OS cells through suppressing miR-26a-5p and that upregulation of FOXO1, identified as a transcription factor of MALAT1, was found to be capable of suppressing MALAT1, thereby inhibiting the proliferation and migration of OS cells. Our results suggested that targeting FOXO1 can be valuable in the therapy of patients with OS.

MATERIALS AND METHODS

Clinical Tissues

The present study was approved by the medical ethics committee of the Affiliated Hospital of Shandong Academy

Address correspondence to Guodong Sun, Department of Traditional Chinese Orthopedics and Traumatology, the Affiliated Hospital of Shandong Academy of Medical Sciences, No. 38 Wuyingshan Road, Jinan, Shandong Province 250031, P.R. China. Tel: 0086-0531-58628811; Fax: 0086-0531-85953187; E-mail: guodongsun_tcot@163.com

of Medical Sciences. Biopsies pathologically diagnosed as OS that met our research requirements were retrieved between January 1, 2012, and December 31, 2016. During this period, 72 fresh OS tissues and their paired normal controls were identified and obtained through biopsy from patients diagnosed with OS in the Department of Traditional Chinese Orthopedics and Traumatology in our hospital. The biopsies (the length of which was ≥0.5 cm in all the cases involved) were stored in liquid nitrogen until use. All the biopsies retrieved were retrospectively reviewed by clinical pathologists who were experts at orthopedic pathology diagnosis and who had no access to the clinical data. All inpatient and outpatient medical records were carefully reviewed. Additional information was obtained by telephoning patients or their relatives whenever required. Comprehensive clinicopathological information, including demographics, TNM stage and grade, T classification, M classification, and follow-up, was obtained in 70 patients. Clinicopathological variables were unavailable in two cases. Informed written consent was obtained from all patients or signed by their relatives with permission before undergoing biopsy detection.

OS Cell Lines

OS cell lines SaoS-2, U2OS, and MG-63 as well as normal osteoblast cell line MCET3-E1 were obtained from (ATCC; Manassas, VA, USA). All the OS cell lines were cultured in RPMI-1640 medium with 10% fetal bovine serum (FBS) in 5% CO_2 humidified air, unless otherwise specified.

Lentiviral Transfection

Lentiviral short hairpin RNA (shRNA) vector as well as shRNA control (shCtrl) vector were commercially serviced by GeneChem Inc. (Shanghai, P.R. China). OS cell lines SaoS-2 and MG-63 were transfected with shCtrl and sh-MALAT1 [multiplicity of infection (MOI) = 100] diluted by Enhanced Infection Solution (ENi.S, pH 7.4). Polybrene (10 μg/ml) was used to enhance the effect of infection. After 72 h of transfection, the density of green fluorescent protein was observed as transfected cells were observed with green fluorescence.

RNA Extract and qRT-PCR

Total RNA from approximately 20 μg of each biopsy sample was extracted using the TRIzol method (Life Technologies, Carlsbad, CA, USA). The resulting RNA was subsequently reverse transcribed into cDNA using a PrimeScript™ 1 First-Strand cDNA Synthesis Kit (Takara, Tokyo, Japan) with MALAT1-specific reversal transcriptional primers. Quantitative real-time- PCR (qRT-PCR) was performed using IQ5 Real-Time System (Bio-Rad, Hercules, CA, USA) with the IQTM SYBR Green Supermix (Bio-Rad) following the accompanying instructions. β-Actin was used as an endogenous loading control for MALAT1 assay and U6 for miR-26a-5p. The relative expression of MALAT1 and miR-26a-5p was calculated using three biological replicates with the $2^{-\Delta\Delta}$Ct approach. Fold changes of relative and normalized expression were calculated with data from CFX Manager 3.0 (Bio-Rad). All the primers involved were designed and synthesized by the GenePharma Company (Shanghai, P.R. China).

Immunoblotting (IB)

Total protein was lysed and harvested from OS cell lines or fresh frozen tissues using strong lysis RIPA buffer (Bioteke, Beijing, P.R. China), followed by quantitation using a Bradford Protein Assay Kit (Bio-Rad). Total protein (30 μg) after quantitation was subjected to 10% SDS-PAGE separation. After transferring the samples to a polyvinylidene fluoride (PVDF) microporous membrane (Millipore, Boston, MA, USA), 5% skim milk powder was used for blocking for 2 h at room temperature. After washing the membrane with Tris-buffered saline with Tween 20, the protein samples were incubated with the polyclonal rabbit anti-human FOXO1 antibody (dilution at 1:1,000; Catalog No. ab39670; Abcam, Cambridge, MA, USA) and monoclonal mouse anti-human β-actin antibody (dilution at 1:5,000; Catalog No. ab197277; Abcam) at 4°C overnight, followed by horseradish peroxidase-conjugated goat anti-mouse IgG secondary antibody (Catalog No. ZDR-5307; Beijing Zhongshan Jinqiao Biotechnology Co., Ltd.) at 4°C overnight. Subsequently, the membranes were visualized by chemiluminescence with SuperSignal West Femto Chemiluminescent Substrate (Thermo Scientific, Waltham, MA, USA), and images were captured with a Bio-Rad camera system (Bio Rad). β-Actin was used as a loading control.

Wound Healing and Transwell Assays

Cell migration ability was assayed using the wound healing method. Transgenic OS cell line MG-63 cells were plated into six-well plates at a concentration of 3×10^5 cells per well and allowed to form a confluent monolayer for 24 h. The monolayer was then scratched with a sterile pipette tip (10 μl), washed with serum-free medium to remove floating and detached cells, and photographed (time 0, 24, 48, and 72 h) by inversion fluorescence microscope (Olympus, Takachiho Seisakusho, Japan). Cell culture inserts (24-well, pore size: 8 μm; BD Biosciences, San Jose, CA, USA) were seeded with 5×10^3 cells in 100 μl of medium with 0.1% FBS. Inserts precoated with Matrigel (40 μl, 1 mg/ml; BD Biosciences) were used for Transwell assays. Medium with 10% FBS (500 μl) was added to the lower chamber and served as a chemotactic agent. Noninvasive cells were wiped from

the upper side of the membrane, and cells on the lower side were fixed in cold methanol (−20°C) and air dried. Cells were stained with 0.1% crystal violet (dissolved in methanol) and counted manually using an inverted microscope. Each individual experiment had triplicate inserts, and four microscopic fields were counted per insert.

Luciferase Reporter Assay

Luciferase reporter assay was performed in MG-63 cells. Cells were plated 1 day before transfection in 24-well plates with a density of 2×10^5 cells per well. miR-26a-5p mimics or its scramble control oligonucleotides (100 nM) and 100 ng of luciferase reporter vector pMIR-REPORT with both wild-type or mutated MALAT1 3′-untranslated region (3′-UTR) were cotransfected into MG-63 cells using Lipofectamine™ 3000. After 48 h, cells were harvested, and relative luciferase activity was measured with the Dual-Luciferase Reporter System (Promega, Madison, WI, USA) on Multimode Reader (Thermo Scientific™, Varioskan™, Flash).

Apoptosis Assay

For apoptotic analysis, the fresh tumor lesions dissected from nude mice were ground into free cells and stained using the Alexa Fluor 488 Annexin-V/Dead Cell Apoptosis Kit with Alexa Fluor 488 Annexin-V and PI for Flow Cytometry (Invitrogen, Carlsbad, CA, USA) following the accompanying protocols.

Chromatin Immunoprecipitation-Quantitative PCR (ChIP-qPCR)

Chromatin was prepared from OS cell line MG-63 following the instructions of the ChIP-qPCR Assay [Catalog No. GPH1002474 (−) 10A; Qiagen, Germany]. Chromatin was fragmented by sonication to produce fragments ranging from 200 to 600 base pairs (bp). Approximately 200 µl of chromatin was used for each immunoprecipitation reaction; 50 µl was then removed from each sample and used as an input control. ChIP was performed using CHIP grade-specific antibody against FOXO1 (Catalog No. ab39670; Abcam). Briefly, ChIP-qPCR was performed with RT-PCR using the SYBR Green method. The reaction consisted in 5 µl of SYBR Green Reaction Mix, 1 µl of 0.1 µM primer pairs, 3 µl of sterile water, and 1 µl of DNA sample (ChIP or Input), for a total volume of 10 µl. Primers were designed to target the transcription start site region and the two flanking regions.

Hematoxylin and Eosin (H&E) Staining

Once the tumor lesions were dissected from xenografted nude mice, they were immediately submerged in 4% paraformaldehyde in PBS at 4°C. After the first week of fixation, the specimens were washed in PBS 0.01 M for 2 days (three washouts per day) followed by normal dehydration in gradient ethanol (70%, 95%, 100%, plus xylol) and then included in paraffin molds to be sectioned with a microtome at the level of the cement–enamel junction in 4-µm slices. The slices were extended in a water bath at 40°C and dried out in a furnace for 1 h at 60°C. The slide sheet was immersed in xylol and absolute gradient ethanol. Staining for histopathological diagnosis and evaluation was performed using H&E.

In Situ Hybridization (ISH)

ISH analysis was performed to detect the expression of MALAT1 and miR-26-5p in tumor lesions dissected from xenografted nude mice. Locked nucleic acid (LNA)-ISH was performed on the slides using the miRCURY LNATM probes against has-miR-26a-5p (Exiqon, Vedbaek, Denmark). The 5′–3′ sequence was UUCAA GUAAUCCAGGAUAGGCU with 5′-DIG and 3′-DIG being labeled, or hybridization with digoxigenin (DIG)-labeled MALAT1 DNA probe 5′-GCATTGGAGATCAG CTTCCGCTAAGATGCTAGCTTGGCCAAGTCTGTT ATGTTCACC-3′ (Shinegene Molecular Biotechnology, Shanghai, P.R. China). The probe was carried out following the manufacturer's protocols. The U6 gene was used as a positive control. Slides were treated with proteinase K (2 µg/ml); 3% H_2O_2 was used to block endogenous peroxidase activity. Hybridization was performed at 52°C overnight with 80 nM of DIG-labeled LNA probes.

Tumor Xenograft Model

All of the animal protocols in the present study were approved by the Medical Experimental Animal Care Commission (MEACC) of Shandong Academy of Medical Sciences, and all the operations on nude mice followed the guidelines given by MEACC. Briefly, female 6- to 8–week-old BALB/c nu/nu mice (Charles River Laboratories, Beijing, P.R. China) were housed in specific pathogen-free conditions. For evaluation of the tumor growth in vivo, 3×10^6 MG-63 cells were suspended in 100 µl of PBS and injected subcutaneously into the flank region of nude mice. Tumor growth was monitored every week, and tumors were measured with fine digital calipers; tumor volume was calculated by the following formula: tumor volume$=0.5\times\text{width}^2\times\text{length}$. Tumor-bearing mice were sacrificed 10 weeks after tumor inoculation, and the tumors were removed, weighed, and separated into two equal parts: one part was used for apoptosis by flow cytometry analysis, and the other was fixed in 3% neutral formalin for ISH and H&E staining.

Statistical Analysis

Statistical analysis was carried out using the SPSS statistical package (Version 17.0; SPSS Inc., Chicago, IL,

USA). Continuous data were described as mean ± SD or median and interquartile range, and categorical variables as percentage. The expression levels of both MALAT1 and miR-26a-5p using qRT-PCR in clinical samples as well as in vitro OS cell lines were analyzed as continuous variables. Because of a nonnormal distribution of expression level of both MALAT1 and miR-26a-5p, Mann–Whitney's nonparametric *U* test was carried out for all values. Kaplan–Meier survival curve was used to evaluate the difference between OS patients with a different level of MALAT1 and miR-26a-5p. A value of $p < 0.05$ was taken to be statistically significant. All the plotting and histograms presented were plotted using the GraphPad Prism software 5.0 version (GraphPad Software Inc., La Jolla, CA, USA).

RESULTS

MALAT1 Was Displayed to be Significantly Upregulated in (Osteosarcoma) Tissues Versus Normal Controls

To investigate the clinicopathological significance of MALAT1 expression, we first detected the expression of MALAT1 at the mRNA level using the qRT-PCR technique in vivo in 70 cases of clinical OS tissue and their normal controls. It was found that MALAT1 was shown to be markedly overexpressed in OS tissues in comparison with normal controls (Fig. 1A), suggesting the oncogenic property of MALAT1 in OS. Subsequently, to test the hypothesis, the detection was extended in vitro in OS cell lines. MALAT1 was also presented to have a pronounced upregulation in OS cell lines (SaoS-2, U2OS, and MG-63) relative to the MC3T3-E1 cell line, a kind of normal osteoblast cell line used as a normal control (Fig. 1B) in our setting. Until now, the expression level of MALAT1 both in clinical tissues and in vitro cell lines of OS indicated its tumor-promoting property. On the basis of the detection of MALAT1 in clinical tissues, we analyzed the clinicopathological significance of MALAT1 expression. It was observed that there was a statistically significant correlation between MALAT1 expression versus distant metastasis and tumor size, whereas no significant difference was observed between MALAT1 expression and other clinical variables other than distant metastasis and tumor size. Furthermore, the Kaplan–Meier survival curve showed that elevated MALAT1 was presented to be significantly associated with poor overall survival of patients with OS (Fig. 1C), suggesting that the MALAT1 expression level was a prognosis-associated factor. To further evaluate the effect exerted over the overall prognosis of OS by MALAT1, multivariate Cox regression analysis was carried out. It was shown that the MALAT1 expression level was an independent prognostic factor in patients with OS. It should be noted here that tumor size and clinical stage were also revealed to be independent prognostic factors. Taken together, the data indicate that the oncogenic properties of MALAT1 and the MALAT1 expression level are independent prognostic factors in OS.

MALAT1 Was Shown to be Significantly Able to Promote Migration, Invasion, and Proliferation of OS Cells

Having understood the clinicopathological significance of MALAT1 expression, subsequently we tried to explore the functional role of MALAT1 in terms of migration in vitro in OS cell lines. Clinicopathological analysis of MALAT1 expression showed that the MALAT1 level was found to be significantly correlated with distant metastasis, which may lead to the implication that MALAT1 is a metastasis-associated gene in OS. Therefore, we primarily focused on the evaluation of the effect it exerted over metastatic variation in OS cells. For one thing, the transgenic OS cell line MG-63 has been established using a lentiviral-based delivery system. Based on this, assessment was made concerning the influence on proliferation of in vitro cell lines using a clonogenic assay. Stable knockdown of MALAT1 was shown to be markedly capable of suppressing the growth of the OS cell line MG-63 in vitro (data not shown). In the following, a Transwell assay showed that knockdown of MALAT1 can significantly prevent the invasive ability of MG-63 cells compared with the control (Fig. 2A), suggesting that MALAT1 itself can promote the invasion of OS cells. Likewise, silencing of MALAT1 was presented to be markedly preventive in the migration of MG-63 cells, as assayed by the wound healing approach (Fig. 2B). The data we obtained in vitro indicated that MALAT1 can enable the motility of OS cells. In order to evaluate its effect over proliferation exerted by MALAT1 in vivo, nude mice xenografted with the OS cell line MG-63 were established in our setting (Fig. 2C). It was discovered that both volume (Fig. 2D) and weight (Fig. 2E) of tumor lesions dissected from mice xenografted with MG-63 whose endogenous MALAT1 was significantly downregulated were found to be remarkably less than that of the control group. To confirm the stable knockdown of MALAT1 in MG-63 cells, the expression level of MALAT1 as well as the identification of tumor lesions were detected using the nucleic acid ISH method and H&E staining, respectively (Fig. 2F). It can be seen that tumor lesions dissected from both experimental and control groups were OSs, and MALAT1 was expectedly and noticeably downregulated compared with the control (Fig. 2F). Moreover, flow cytometric analysis of fresh cells from tumor lesions dissected from nude mice showed that knockdown of MALAT1 was presented to be able to significantly induce apoptosis versus control (Fig. 2G). The data we obtained from xenografted nude mice indicated that MALAT1 can promote proliferation of OS cells in vivo.

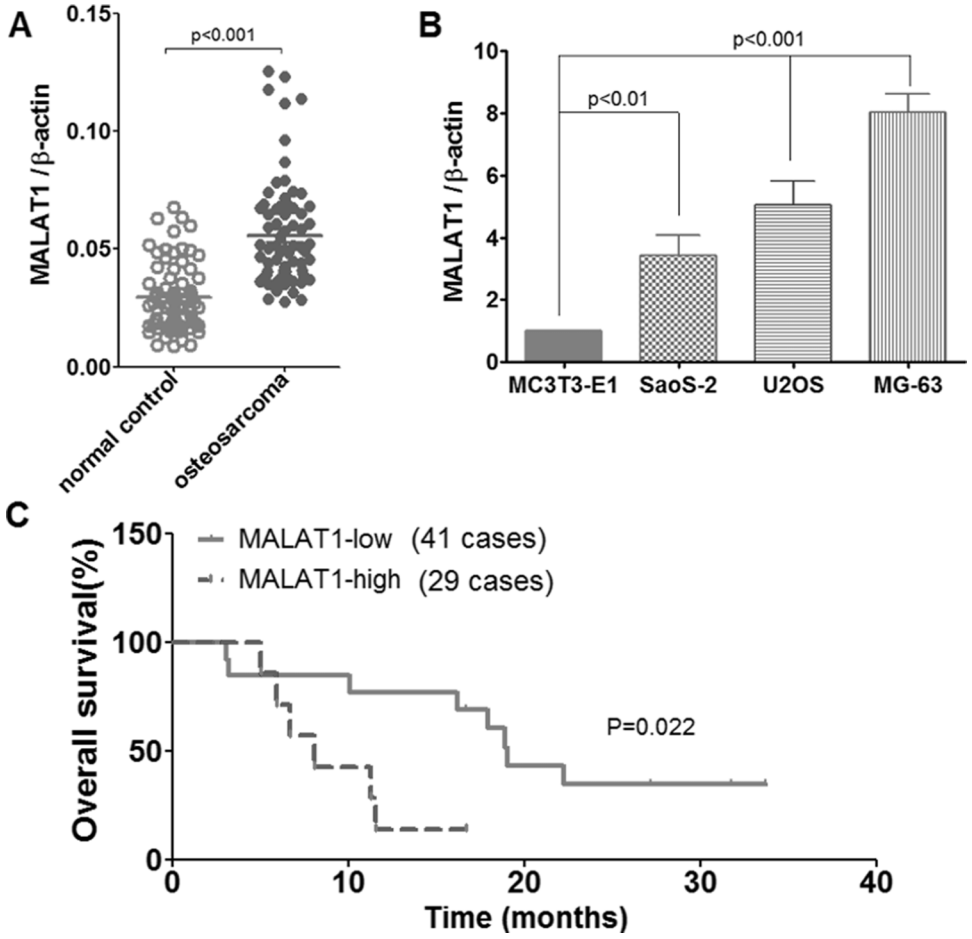

Figure 1. MALAT1 (metastasis-associated lung adenocarcinoma transcript 1) was shown to be markedly overexpressed in osteosarcoma (OS) tissues as well as in cell lines compared to their normal controls. (A) MALAT1 was shown to be significantly upregulated in OS tissues versus paired normal controls. Detection was carried out in 72 cases of OS and its normal controls using the quantitative real-time polymerase chain reaction (qRT-PCR) approach, and relative expression of MALAT1 was calculated using the $2^{-\Delta\Delta}$CT method. β-Actin was used as internal loading control. (B) Similarly, MALAT1 was found to be remarkably upregulated in OS cell lines (SaoS-2, U2OS, and MG-63) in comparison with the normal osteoblast cell line MC3T3-E1. (C) Elevated MALAT1 was discovered to be noticeably associated with poor overall survival of patients with OS. The median value (6.26) of MALAT1 expression in patients with OS was selected as cutoff in our analysis of prognosis. OS patients enrolled whose MALAT1 expression was shown to be equal to or above the cutoff we set were defined as MALAT1 high expression (41 cases), whereas those whose MALAT1 expression was detected to be below the cutoff value we set were defined as MALAT1 low expression (29 cases). Log-rank test was used to statistically analyze the difference of prognosis. As for relative expression of MALAT1, *p* values were calculated using the Mann–Whitney *U* tests (unpaired, two-tailed) in comparison with the control group, whereas *p* value was calculated using log-rank test (GraphPad Prism 5.0 version) when it comes to statistical analysis of survival difference.

FOXO1 Was Identified to be Able to Negatively Regulate MALAT1 in OS Cells

We then asked why MALAT1 was upregulated in OS. To explore the underlying regulatory mechanism behind MALAT1, we performed bioinformatic analysis of the sequence of MALAT1. It was found that there has been a potential binding site of transcriptional factor forkhead box O1 (FOXO1) existing on the promoter of MALAT1 sequence. To confirm the bioinformatic prediction, a luciferase reporter assay as well as CHIP-qPCR were used. Upstream from −450 to −600 bp of the promoter sequence of MALAT1 was shown to be significantly capable of binding with FOXO1 (Fig. 3A), as exemplified by luciferase reporter assay. To further verify the direct binding of FOXO1 on the promoter of MALAT1, we detected the relative expression of the fragmented DNA on the promoter of MALAT1 using CHIP-qPCR after transfection with specific small interference RNA (siRNA) against the predicted binding site of FOXO1 (GTAAACA). It was confirmed that FOXO1 was able to directly bind with the promoter of MALAT1 compared with control (Fig. 3B). Based on this observation, we made clear the

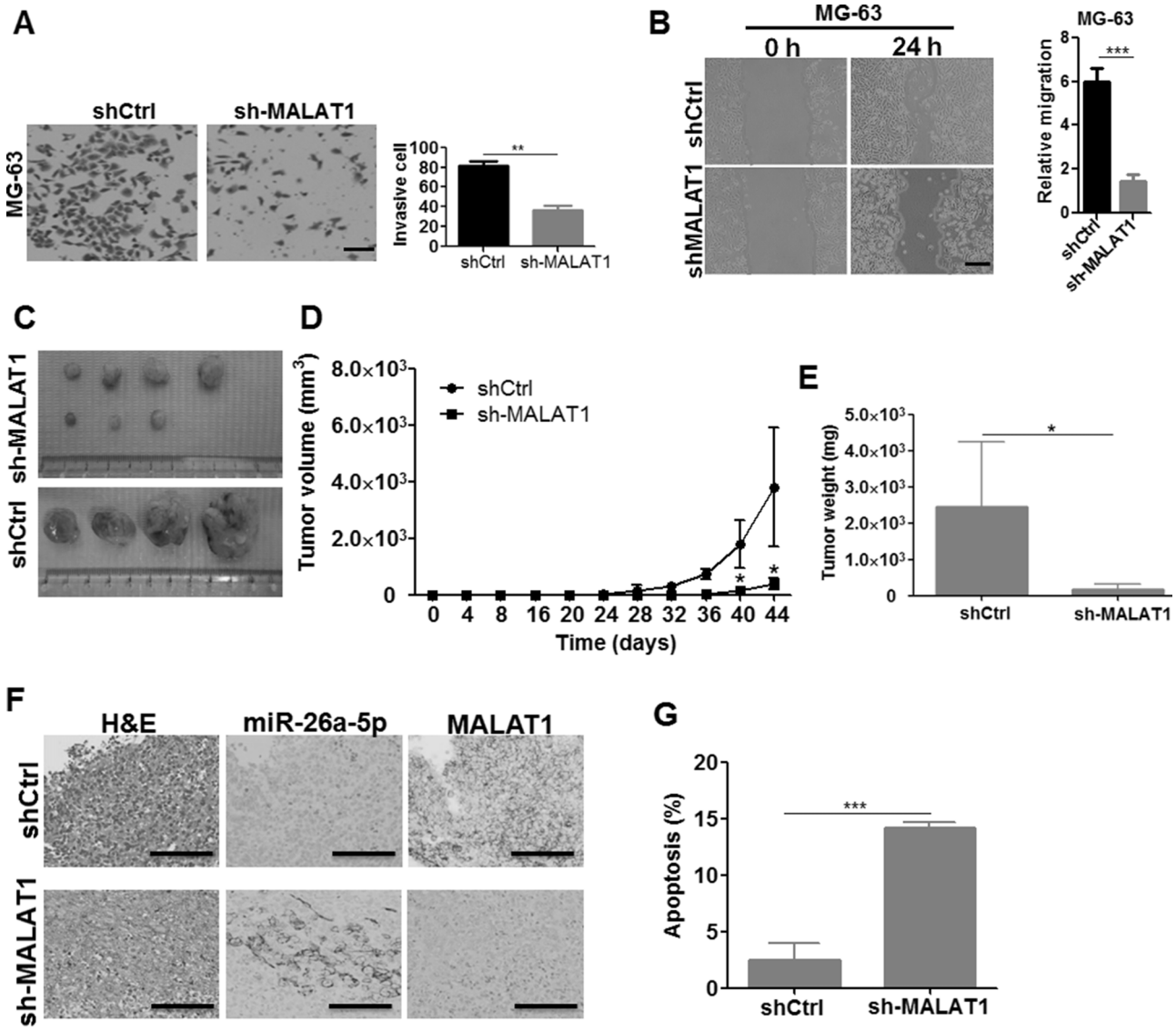

Figure 2. MALAT1 was shown to be able to promote migration, invasion, and proliferation of MG-63 cells. (A) With the help of Transwell assay, knockdown of MALAT1 was presented to be capable of preventing the invasive ability in OS cell line MG-63. (B) Likewise, knockdown of MALAT1 was shown to be able to prevent migration in MG-63 after wound healing assay. (C) Shown are tumor lesions of nude mice xenografted with MG-63 cells whose endogenous MALAT1 was stably knocked down (labeled as sh-MALAT1, $n=7$) and MG-63 cells whose MALAT1 was hardly changed (labeled as sh-Ctrl, $n=4$). (D) The tumor volume of tumor lesions dissected from nude mice. (E) Similarly, the tumor weight of lesions after being dissected from nude mice was also analyzed. (F) Expression of MALAT1 and miR-26a-5p was confirmed in tumor lesions after being dissected using in situ hybridization method. (G) Apoptotic assay was performed using the flow cytometry approach as soon as the tumor lesions were dissected from its holders. Of note here, as for Transwell and wound healing assays, shown are representative figures from three different independent replicates. The p value was calculated using Mann–Whitney U tests (unpaired, two tailed: $*p<0.05$, $**p<0.01$, $***p<0.001$) in comparison with the control group.

basal level of FOXO1 at the protein level in OS cell lines SaoS-2, U2OS, and MG-63 cells (Fig. 3C). Meanwhile, we evaluated the transient knockdown of FOXO1 at the protein level using specific siRNA in these three OS cell lines (Fig. 3C and D). Following the successful transient knockdown of FOXO1 in MG-63 cells (Fig. 3E), we assayed the expression variation of MALAT1 as well as miR-26a-5p, a putative binding target of MALAT1. It was presented that MALAT1 was noticeably upregulated after FOXO1 was successfully and stably knocked down in MG-63 cells. On the contrary, miR-26a-5p was significantly downregulated (Fig. 3F). In the clinical tissue level, FOXO1 was also confirmed to be remarkably downregulated in OS tissues compared with normal controls (data not shown), suggesting that FOXO1 acted as a tumor suppressor in OS tissues as well as in cell lines.

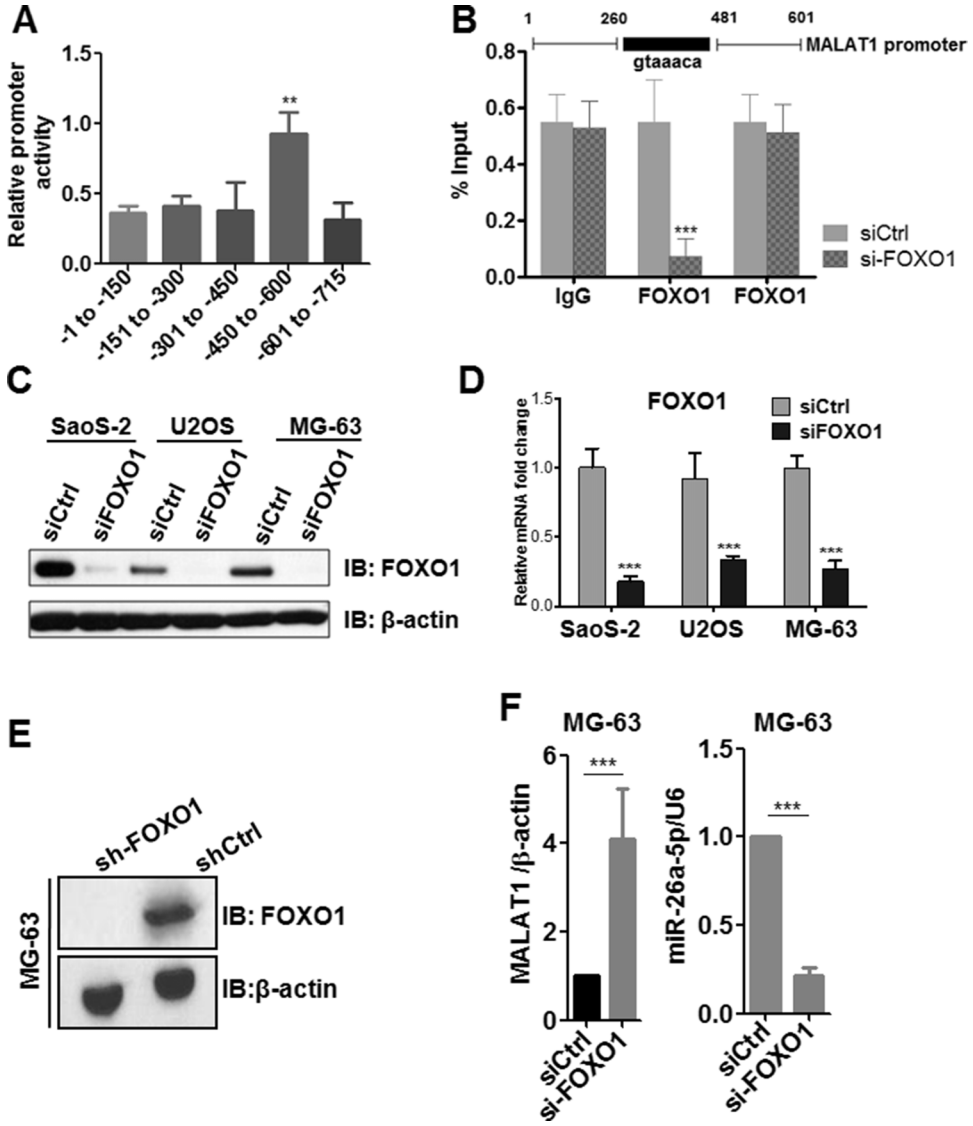

Figure 3. Transcriptional factor forkhead box O1 (FOXO1) was identified to negatively regulate MALAT1 expression in OS cells. (A) FOXO1 was found to directly bind with the promoter of MALAT1 using the chromatin immunoprecipitation (CHIP)-qPCR method. (B) FOXO1 was confirmed to directly bind with the promoter of MALAT1 using CHIP-qPCR at –467 base pair (bp), upstream of the promoter of MALAT1. (C) Transient silencing effect as well as basal expression of FOXO1 in OS cell lines SaoS-2, U2OS, and MG-63 at protein level after transfection with specific siRNA against FOXO1. β-Actin was used as an internal loading control. (D) Quantitative analysis of immunoblotting (IB) of FOXO1. (E) Knockdown of FOXO1 at protein level using short hairpin RNA (shRNA) technique in MG-63 cells, detected by IB. (F) On the basis of successful knockdown of FOXO1 in MG-63 cells, mRNA variation of MALAT1 as well as miR-26a-5p was monitored using qRT-PCR. Shown here are representative figures from three different independent replicates, and the *p* value was calculated using Mann–Whitney *U* tests (unpaired, two tailed: $^{**}p<0.01$, $^{***}p<0.001$) versus control.

These data demonstrate that FOXO1 can directly bind with the promoter of MALAT1, thereby negatively regulating the expression of MALAT1.

miR-26a-5p Was Shown to be Able to be Negatively and Directly Regulated by MALAT1 in OS Cells

Subsequent to the finding that FOXO1 was capable of negatively regulating MALAT1, we next asked how MALAT1 promoted the motility of OS cells. In consideration that MALAT1 was an lncRNA, which was proposed to play a regulatory role and which itself could not likely directly engage in the malignant behaviors of cancer cells, consequently we tried to figure out the underlying downstream target of MALAT1. With the help of the online bioinformatic prediction tool (http://www.microrna.org/microrna/), the MALAT1 sequence was found to have

four putative binding sites for miR-26a-5p. The underlying binding site of miR-26a-5p was bioinformatically predicted to be 464 bp on the sequence of MALAT1 (Fig. 4A). To confirm the bioinformatic prediction, a luciferase reporter assay was employed in MG-63 cells. It was found that MALAT1 was directly able to bind with miR-26a-5p (Fig. 4B) in MG-63 cells, indicating that MALAT1 can directly regulate miR-26a-5p. Next, we detected the expression level of miR-26a-5p in the same clinical cohort where MALAT1 was detected. miR-26a-5p was shown to be remarkably downregulated in OS tissues compared with the normal control (Fig. 4C). In order to verify the correlation between MALAT1 and miR-26a-5p on the clinical tissue level, the Pearson correlation was conducted. It showed that there was a significantly inverse correlation between MALAT1 and miR-26a-5p expression (Fig. 4D), confirming what we observed using the luciferase reporter assay on in vitro cell lines. Moreover, the Kaplan–Meier

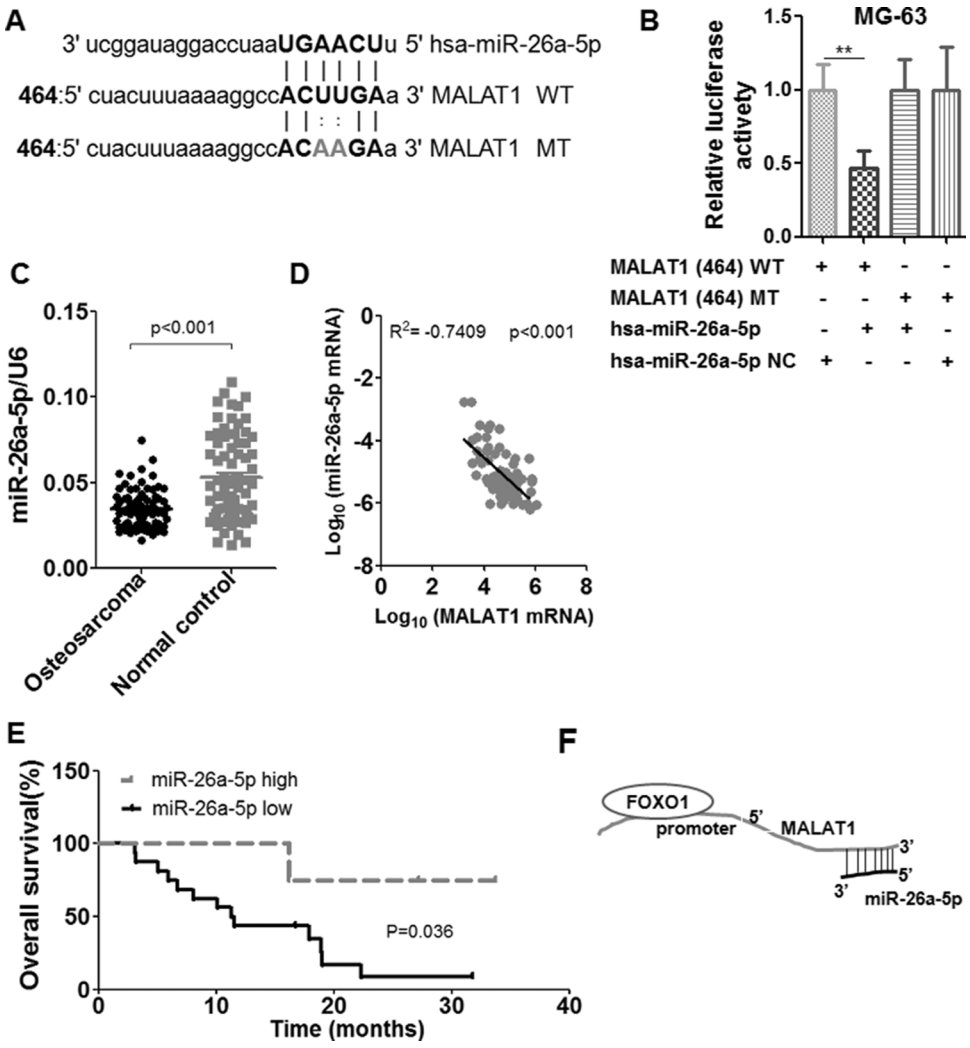

Figure 4. miR-26a-5p was identified to be directly and negatively regulated by MALAT1 in OS cells. (A) miR-26a-5p was bioinformatically predicted to be a putative binding target of MALAT1 using an online bioinformatic tool (http://www.microrna.org/microrna/). (B) miR-26a-5p was confirmed to be a binding target of MALAT1 using luciferase reporter assay in MG-63 cells. (C) miR-26a-5p was shown to be prominently downregulated in OS tissues compared with its normal control. (D) Pearson correlation analysis showed that there was an inversed correlation between expression of MALAT1 and miR-26a-5p in the same cohort. (E) Elevated expression of miR-26a-5p was found to be significantly associated with better overall survival of patients with OS. The median value of miR-26a-5p expression was chosen as the cutoff. Those whose miR-26a-5p expression was equal to or above the cutoff were defined as high expression, whereas those whose expression was below the cutoff were defined as low expression. (F) Schematic diagram of the working model of MALAT1 in the study, promotion of invasion and migration of OS cells by MALAT1, can be negatively regulated by FOXO1 and was shown to be able to directly and negatively regulate miR-26a-5p. The p value was worked out through Mann–Whitney U tests (unpaired, two tailed: $^{**}p < 0.01$) compared with control.

survival analysis showed that the decreased miR-26a-5p level was markedly associated with inferior overall survival of patients with OS (Fig. 4E).

DISCUSSION

This is the first report to show that MALAT1 exerts its oncogenic role through suppressing miR-26a-5p and that FOXO1 can directly regulate MALAT1 through promoter binding in OS, suggesting that upregulation of FOXO1 could be a novel therapeutic alternative for the treatment of patients with OS. Our study supports the theory that restoration of FOXO1 could be used as an ideal therapeutic strategy in the setting of OS. FOXO1 has been reported to play a tumor suppressing role in OS; nevertheless, the molecular mechanism by which FOXO1 works remains to be studied. Our study provides an alternative possible mechanism through which FOXO1 inhibits the malignant behaviors of OS cells.

An original report showed that MALAT1 in the setting of tumors came from liver cancer where the MALAT1 gene was shown to be significantly upregulated compared with paired normal controls[10]. This was extensively extended in other types of cancers, generally speaking, including solid[11–13] and nonsolid tumors[14]. Observations from these earlier studies that certain types of tumors were detected to have elevated levels of MALAT1, which was shown to be markedly correlated with tumor grade and prognosis[13,15,16], suggest that MALAT1 could serve as an oncogenic lncRNA mediating malignant behaviors in tumor initiation, progression, metastasis, chemoresistance, and recurrence[17]. In the background of OS, MALAT1 was found not only to play an important role in the tumorigenesis of OS[18] but also to be able to promote proliferation, migration, and invasion of OS cells[8,19]. It has been reviewed[6] and meta-analyzed[20] that MALAT1 can be used to predict both metastasis and prognosis, which was totally in support of our own observations. These findings lead to the suggestion that MALAT1 could be used as an ideal therapeutic target for patients with OS[9]. Despite this fact, the mechanism through which MALAT1 plays a role in tumors, not to mention OS, remains unknown and needs to be clarified. A recent study concerning MALAT1 in OS from a signal pathway regulation aspect showed that MALAT1 could promote the proliferation and metastasis of OS cells by activating the PI3K/Akt pathway[8]. No other mechanistic study with respect to MALAT1 has appeared regarding OS. In contrast, there have been several mechanistic studies regarding MALAT1 in other types of cancers. Li et al. found that MALAT1 exerts oncogenic functions by targeting miR-204 in lung adenocarcinoma[13]. Similarly, miR-206[21] and miR-1[22,23] were also identified to be another downstream target of miRNAs that can be directly regulated by MALAT1 in gallbladder cancer and breast cancer. In addition, miR-101 and miR-217 were demonstrated to be able to regulate MALAT1 in esophageal squamous cell carcinoma[24]. In another recent study, MALAT1 was shown to be able to interact with miR-205 in renal cell carcinoma[25], thereby promoting aggressiveness. In the literature mentioned above, although the relevant miRNAs were shown to be able to regulate or be regulated by MALAT1, they have not been reported or found in the setting of OS. Furthermore, the reason that MALAT1 was displayed to be significantly upregulated in OS remains elusive.

miR-26a, despite being somewhat controversial in cancers[26], has been found to be consistently downregulated in OS by different groups[27–29], with the exception of one recent study[30] in which the finding was that miR-26a was upregulated in OS tissues as well as in vitro in OS cell lines. This was in stark contrast with the observation that miR-26a was shown to be downregulated in OS in other studies[27–29]. The possible reasons leading to this discrepancy remain unknown. However, it may be due to the technical aspects, including a different detection method and the clinical samples involved, a different cutoff value chosen leading to a different outcome, and so on. However, from these observations, there is an implication that miR-26a could play a tumor suppressing role in OS. Restoration of miR-26a could suppress the growth and metastasis of OS cells[29]. Although the impact of miR-26a on a functional phenotype has been reported in OS, the reason why miR-26a stays downregulated in OS remains largely unknown, other than two reports[31,32] stating that a promoter of miR-26a had heavily undergone hypermethylation in breast cancer, which could account for the reason that miR-26a was shown to be downregulated. In our study, we show for the first time that miR-26a-5p was directly suppressed by MALAT1 through 3′-UTR binding in OS. In other words, MALAT1 was shown to negatively regulate miR-26a-5p. Our results could alternatively account for the phenomenon of why miR-26a-5p was observed to be significantly downregulated in OS tissues as well as cell lines, other than the proposal that miR-26a promoter underwent hypermethylation[31,32].

Given that the reason MALAT1 was shown to be significantly upregulated in OS remains unknown, we used the ChIP-qPCR approach to identify the unknown transcription factor regulating MALAT1. FOXO1 was identified as a regulatory transcription factor for MALAT1, and FOXO1 was shown to negatively regulate the transcription of MALAT1. To confirm the result, a variation of MALAT1 was detected using qRT-PCR after FOXO1 was artificially up- or downregulated using transfection with vectors harboring full-length cDNA or shRNA sequence. It turns out that MALAT1 was markedly decreased as FOXO1 was upregulated, and it is quite opposite when FOXO1 was silenced. Despite FOXO1 being identified

as a negative regulatory transcription factor for MALAT1, the precise binding site of FOXO1 on the promoter of MALAT1 remains to be investigated. Based on our study that FOXO1 was shown to negatively regulate MALAT1, which negatively regulated miR-26a-5p, together with previously relevant reports[33,34] that FOXO1 was shown to inhibit OS oncogenesis, we postulated that restoration of FOXO1 could lead to the upregulation of miR-26a-5p through negative regulation of MALAT1. Accordingly, we used methylseleninic acid (MSA), an activator of FOXO1, to treat OS cell lines. It was found that miR-26a-5p was remarkably upregulated in OS cells treated with MSA, together with decreased MALAT1 (data not shown), which substantiates our postulation. Our findings are not meant to suggest that FOXO1 is the only transcriptional factor regulating MALAT1, but we show that FOXO1 has the capacity to directly regulate MALAT1, thereby regulating miR-26a-5p.

In summary, we show that FOXO1 suppresses growth and migration through negative regulation of MALAT1, which regulates miR-26a-5p in OS, suggesting that upregulation of FOXO1 could be used as an alternative therapeutic strategy for patients with OS. Our result supports the suitability of FOXO1 in the treatment of OS.

ACKNOWLEDGMENT: The present study was supported by the Department of Traditional Chinese Orthopedics and Traumatology, The Affiliated Hospital of Shandong Academy of Medical Sciences. The authors declare no conflicts of interest.

REFERENCES

1. Anderson ME. Update on survival in osteosarcoma. Orthop Clin North Am. 2016;47:283–92.
2. Wan J, Zhang X, Liu T, Zhang X. Strategies and developments of immunotherapies in osteosarcoma. Oncol Lett. 2016;11:511–20.
3. Bishop MW, Janeway KA, Gorlick R. Future directions in the treatment of osteosarcoma. Curr Opin Pediatr. 2016;28: 26–33.
4. Scott MC, Sarver AL, Gavin KJ, Thayanithy V, Getzy DM, Newman RA, Cutter GR, Lindblad-Toh K, Kisseberth WC, Hunter LE, Subramanian S, Breen M, Modiano JF. Molecular subtypes of osteosarcoma identified by reducing tumor heterogeneity through an interspecies comparative approach. Bone 2011;49:356–67.
5. Kushlinskii NE, Fridman MV, Braga EA. Molecular mechanisms and microRNAs in osteosarcoma pathogenesis. Biochem Biokhimiia 2016;81:315–28.
6. Li Z, Yu X, Shen J. Long non-coding RNAs: Emerging players in osteosarcoma. Tumour Biol. 2016;37:2811–6.
7. Huynh NP, Anderson B, Guilak F, McAlinden A. Emerging roles for long non-coding RNAs in skeletal biology and disease. Connect Tissue Res. 2017;58:116–41.
8. Dong Y, Liang G, Yuan B, Yang C, Gao R, Zhou X. MALAT1 promotes the proliferation and metastasis of osteosarcoma cells by activating the PI3K/Akt pathway. Tumour Biol. 2015;36:1477–86.
9. Cai X, Liu Y, Yang W, Xia Y, Yang C, Yang S, Liu X. Long noncoding RNA MALAT1 as a potential therapeutic target in osteosarcoma. J Orthop Res. 2016;34:932–41.
10. Luo JH, Ren B, Keryanov S, Tseng GC, Rao UN, Monga SP, Strom S, Demetris AJ, Nalesnik M, Yu YP, Ranganathan S, Michalopoulos GK. Transcriptomic and genomic analysis of human hepatocellular carcinomas and hepatoblastomas. Hepatology 2006;44:1012–24.
11. Mendell JT. Targeting a long noncoding RNA in breast cancer. N Engl J Med. 2016;374:2287–9.
12. Ma J, Wang P, Yao Y, Liu Y, Li Z, Liu X, Li Z, Zhao X, Xi Z, Teng H, Liu J, Xue Y. Knockdown of long noncoding RNA MALAT1 increases the blood-tumor barrier permeability by up-regulating miR-140. Biochim Biophys Acta 2016;1859:324–38.
13. Li J, Wang J, Chen Y, Li S, Jin M, Wang H, Chen Z, Yu W. LncRNA MALAT1 exerts oncogenic functions in lung adenocarcinoma by targeting miR-204. Am J Cancer Res. 2016;6:1099–107.
14. Ronchetti D, Agnelli L, Taiana E, Galletti S, Manzoni M, Todoerti K, Musto P, Strozzi F, Neri A. Distinct lncRNA transcriptional fingerprints characterize progressive stages of multiple myeloma. Oncotarget 2016;7:14814–30.
15. Meseure D, Vacher S, Lallemand F, Alsibai KD, Hatem R, Chemlali W, Nicolas A, De Koning L, Pasmant E, Callens C, Lidereau R, Morillon A, Bieche I. Prognostic value of a newly identified MALAT1 alternatively spliced transcript in breast cancer. Br J Cancer 2016;114:1395–404.
16. Li Y, Yang Z, Wan X, Zhou J, Zhang Y, Ma H, Bai Y. Clinical prognostic value of metastasis-associated lung adenocarcinoma transcript 1 in various human cancers: An updated meta-analysis. Int J Biol Markers 2016;31:e173–82.
17. Jiao F, Hu H, Han T, Yuan C, Wang L, Jin Z, Guo Z, Wang L. Long noncoding RNA MALAT-1 enhances stem cell-like phenotypes in pancreatic cancer cells. Int J Mol Sci. 2015;16:6677–93.
18. Taniguchi M, Fujiwara K, Nakai Y, Ozaki T, Koshikawa N, Toshio K, Kataba M, Oguni A, Matsuda H, Yoshida Y, Tokuhashi Y, Fukuda N, Ueno T, Soma M, Nagase H. Inhibition of malignant phenotypes of human osteosarcoma cells by a gene silencer, a pyrrole-imidazole polyamide, which targets an E-box motif. FEBS Open Bio 2014;4: 328–34.
19. Fang D, Yang H, Lin J, Teng Y, Jiang Y, Chen J, Li Y. 17beta-estradiol regulates cell proliferation, colony formation, migration, invasion and promotes apoptosis by upregulating miR-9 and thus degrades MALAT-1 in osteosarcoma cell MG-63 in an estrogen receptor-independent manner. Biochem Biophys Res Commun. 2015;457:500–6.
20. Zhu L, Liu J, Ma S, Zhang S. Long noncoding RNA MALAT-1 can predict metastasis and a poor prognosis: A meta-analysis. Pathol Oncol Res. 2015;21:1259–64.
21. Wang SH, Zhang WJ, Wu XC, Zhang MD, Weng MZ, Zhou D, Wang JD, Quan ZW. Long non-coding RNA Malat1 promotes gallbladder cancer development by acting as a molecular sponge to regulate miR-206. Oncotarget 2016;7:37857–67.
22. Jin C, Yan B, Lu Q, Lin Y, Ma L. Reciprocal regulation of Hsa-miR-1 and long noncoding RNA MALAT1 promotes triple-negative breast cancer development. Tumour Biol. 2016;37:7383–94.
23. Chou J, Wang B, Zheng T, Li X, Zheng L, Hu J, Zhang Y, Xing Y, Xi T. MALAT1 induced migration and

invasion of human breast cancer cells by competitively binding miR-1 with cdc42. Biochem Biophys Res Commun. 2016;472:262–9.
24. Wang X, Li M, Wang Z, Han S, Tang X, Ge Y, Zhou L, Zhou C, Yuan Q, Yang M. Silencing of long noncoding RNA MALAT1 by miR-101 and miR-217 inhibits proliferation, migration, and invasion of esophageal squamous cell carcinoma cells. J Biol Chem. 2015;290:3925–35.
25. Hirata H, Hinoda Y, Shahryari V, Deng G, Nakajima K, Tabatabai ZL, Ishii N, Dahiya R. Long noncoding RNA MALAT1 promotes aggressive renal cell carcinoma through Ezh2 and interacts with miR-205. Cancer Res. 2015;75: 1322–31.
26. Chen J, Zhang K, Xu Y, Gao Y, Li C, Wang R, Chen L. The role of microRNA-26a in human cancer progression and clinical application. Tumour Biol. 2016;37:7095–108.
27. Song QC, Shi ZB, Zhang YT, Ji L, Wang KZ, Duan DP, Dang XQ. Downregulation of microRNA-26a is associated with metastatic potential and the poor prognosis of osteosarcoma patients. Oncol Rep. 2014;31:1263–70.
28. Tan X, Fan S, Wu W, Zhang Y. MicroRNA-26a inhibits osteosarcoma cell proliferation by targeting IGF-1. Bone Res. 2015;3:15033.
29. Lu J, Song G, Tang Q, Yin J, Zou C, Zhao Z, Xie X, Xu H, Huang G, Wang J, Lee DF, Khokha R, Yang H, Shen J. MiR-26a inhibits stem cell-like phenotype and tumor growth of osteosarcoma by targeting Jagged1. Oncogene 2017; 36:231–41.
30. Qu F, Li CB, Yuan BT, Qi W, Li HL, Shen XZ, Zhao G, Wang JT, Liu YJ. MicroRNA-26a induces osteosarcoma cell growth and metastasis via the Wnt/beta-catenin pathway. Oncol Lett. 2016;11:1592–6.
31. Sandhu R, Rivenbark AG, Mackler RM, Livasy CA, Coleman WB. Dysregulation of microRNA expression drives aberrant DNA hypermethylation in basal-like breast cancer. Int J Oncol. 2014;44:563–72.
32. Borno ST, Fischer A, Kerick M, Falth M, Laible M, Brase JC, Kuner R, Dahl A, Grimm C, Sayanjali B, Isau M, Röhr C, Wunderlich A, Timmermann B, Claus R, Plass C, Graefen M, Simon R, Demichelis F, Rubin MA, Sauter G, Schlomm T, Sültmann H, Lehrach H, Schweiger MR. Genome-wide DNA methylation events in TMPRSS2-ERG fusion-negative prostate cancers implicate an EZH2-dependent mechanism with miR-26a hypermethylation. Cancer Discov. 2012;2:1024–35.
33. Guan H, Tan P, Xie L, Mi B, Fang Z, Li J, Yue J, Liao H, Li F. FOXO1 inhibits osteosarcoma oncogenesis via Wnt/beta-catenin pathway suppression. Oncogenesis 2015;4: e166.
34. Niedan S, Kauer M, Aryee DN, Kofler R, Schwentner R, Meier A, Pötschger U, Kontny U, Kovar H. Suppression of FOXO1 is responsible for a growth regulatory repressive transcriptional sub-signature of EWS-FLI1 in Ewing sarcoma. Oncogene 2014;33:3927–38.